

This article was downloaded by:

On: 25 January 2011

Access details: *Access Details: Free Access*

Publisher *Taylor & Francis*

Informa Ltd Registered in England and Wales Registered Number: 1072954 Registered office: Mortimer House, 37-41 Mortimer Street, London W1T 3JH, UK



Liquid Crystals

Publication details, including instructions for authors and subscription information:

<http://www.informaworld.com/smpp/title~content=t713926090>

Rod-shaped dopants for flexoelectric nematic mixtures

Nayyar Aziz^a; Stephen M. Kelly^a; Warren Duffy^b; Mark Goulding^b

^a Department of Chemistry, University of Hull, Hull, UK ^b Merck Chemicals Ltd, Chilworth Technical Centre, University Parkway, Southampton, UK

Online publication date: 05 November 2010

To cite this Article Aziz, Nayyar , Kelly, Stephen M. , Duffy, Warren and Goulding, Mark(2009) 'Rod-shaped dopants for flexoelectric nematic mixtures', *Liquid Crystals*, 36: 5, 503 – 520

To link to this Article: DOI: 10.1080/02678290903031643

URL: <http://dx.doi.org/10.1080/02678290903031643>

PLEASE SCROLL DOWN FOR ARTICLE

Full terms and conditions of use: <http://www.informaworld.com/terms-and-conditions-of-access.pdf>

This article may be used for research, teaching and private study purposes. Any substantial or systematic reproduction, re-distribution, re-selling, loan or sub-licensing, systematic supply or distribution in any form to anyone is expressly forbidden.

The publisher does not give any warranty express or implied or make any representation that the contents will be complete or accurate or up to date. The accuracy of any instructions, formulae and drug doses should be independently verified with primary sources. The publisher shall not be liable for any loss, actions, claims, proceedings, demand or costs or damages whatsoever or howsoever caused arising directly or indirectly in connection with or arising out of the use of this material.

Rod-shaped dopants for flexoelectric nematic mixtures

Nayyar Aziz^a, Stephen M. Kelly^{a*}, Warren Duffy^b and Mark Goulding^b

^aDepartment of Chemistry, University of Hull, Cottingham Rd, Hull HU6 7RX, UK; ^bMerck Chemicals Ltd, Chilworth Technical Centre, University Parkway, Southampton SO16 7QD, UK

(Received 3 September 2008; final form 8 May 2009)

We report the synthesis and liquid crystalline behaviour of two series of *para*-substituted terphenyls as dopants with a rigid rod-like shape, rather than a wedge-, pear- or banana-shape, for guest–host nematic mixtures with flexoelectric properties. One series of liquid crystalline dopants is of low-to-strongly negative dielectric anisotropy and the other is of low-to-strongly positive dielectric anisotropy. The usefulness of apolar and polar rod-like dopants as components of flexoelectric nematic mixtures of positive dielectric anisotropy for use in LCDs is investigated in general and the dependence of the flexoelectric properties of the doped nematic mixtures on the polarity of the dopants is studied in particular. The correlation between the concentration of the dopant and the magnitude of the flexoelastic ratio of several guest–host nematic mixtures is investigated.

Keywords: polyfluorinated dopants; flexoelectric nematics; terphenyls

1. Introduction

R. B. Meyer postulated in 1969 that splay and bend deformations of the director field of a nematic phase constituted of molecules with shape polarity and a permanent dipole would induce a flexoelectric polarisation in the nematic phase and this polarisation could be coupled to an applied electric field to facilitate new kinds of liquid crystal display (LCD) (1). It was also postulated that wedge-, pear- or banana-shaped molecules, rather than the classic rod-like or lath-like shape of calamitic nematic liquid crystals, would be required to induce these effects, e.g. pear-shaped molecules should pack efficiently to create a splay conformation. This bulk splay conformation should induce a preferred direction of the molecular dipole moment and a local polarisation of the nematic phase (1–4). The resultant spontaneous polarisation orientates along the longitudinal part of the molecules, i.e. parallel to the nematic director, if the pear-shaped molecules align with the thick ends of the molecules in the direction of the splay. A combination of splay and bend deformations should induce a flexoelectric polarisation of a nematic phase made up of wedge- or pear-drop shaped molecules, see Figure 1 (1, 2).

The flexoelectric polarisation, \mathbf{P} , of such a nematic phase may be represented as

$$\mathbf{P} = e_1 \mathbf{n}(\nabla \cdot \mathbf{n}) + e_3 \mathbf{n} \times (\nabla \times \mathbf{n})$$

where e_1 and e_3 are the flexoelectric coefficients related to the splay and bend deformations and \mathbf{n} is the nematic director. LCDs based on the flexoelectric effect in either a chiral nematic phase (5–9) or a nematic phase (10–12)

may exhibit bistability, ultra-fast switching, high optical contrast and recovery from mechanical distortion. A novel electro-optic display device based on the in-plane switching flexoelectric response of a nematic liquid crystal to electric fields in the plane of the display was reported in 1987 (5). It has since been further developed further as the Uniform-Lying Helix (UHL)-LCD (6–8). This type of LCD involves the displacement of the optic axis of a chiral nematic phase acting as uniaxial birefringent plate in the stripe texture in the plane of the cell. At low electric field strength it utilises the flexoelectric coupling with the applied field. This is a linear electro-optical effect. It is particularly attractive due to the good optical properties of in-plane switching, the presence of grey scale, the temperature independence of the optical response over a wide temperature range (0–50°C) and the very short response times ($\tau < 100 \mu\text{s}$). A number of surface-switched, as opposed to volume-switched, bistable nematic and chiral nematic LCDs, including the BiNem[®]-LCD (9, 10) and the bistable nematic Zenithal Bistable Display (ZBD) (11, 12) have reported. The switching between two equally stable states present in both the BiNem[®]-LCD and the ZBD is also achieved by flexoelectric coupling with the electric field applied to the nematic liquid crystal mixture in the device. Both of these types of bistable LCDs use crossed polarisers to generate an optical contrast between the two bistable states. The BiNem[®]-LCD switches between a non-twisted nematic state and a 180° twisted nematic state by the application of an electric field above the threshold value required to break the surface anchoring in one of the states of the nematic phase on a simple monostable alignment layer

*Corresponding author. Email: s.m.kelly@hull.ac.uk

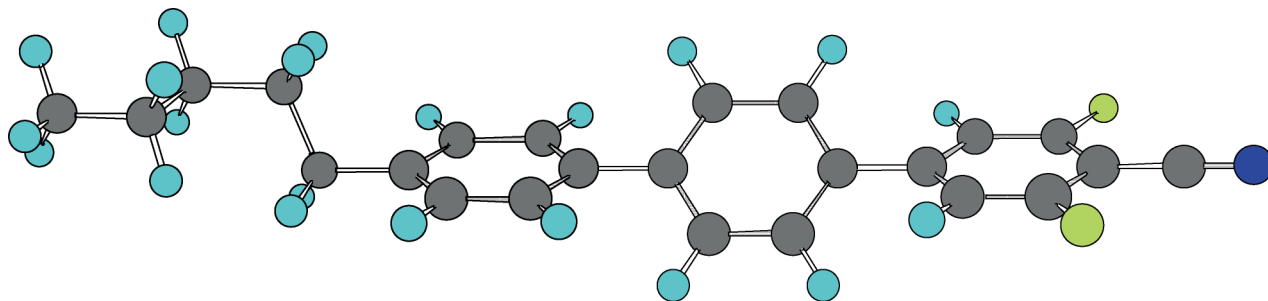


Figure 1. (Colour online). A model of 4-cyano-3,5-difluoro-4''-pentyl-*p*-terphenyl (**25**) as modelled using ChemDraw Pro 3D software.

(9, 10). The BiNem[®]-LCD exhibits high contrast, a large viewing angle, short switching times and grey scale. The ZBD incorporates surfactant-coated grating surfaces with a homeotropic alignment at each surface. Two stable pretilt configurations are possible with a high or a low pretilt as long as the groove depth to the pitch ratio of the grating is optimised (11, 12). The ZBD exhibits fast switching times, memory, shock stability and high contrast ratio. It makes use of the electric field-induced breaking of the surface anchoring between a high pre-tilt state and a low pre-tilt state of equal energy to induce very short response times. The ZBD also has the additional advantage of complete recovery from direct substantial mechanical distortion as long as the substrate surfaces are not brought into direct contact.

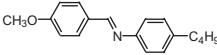
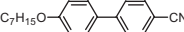
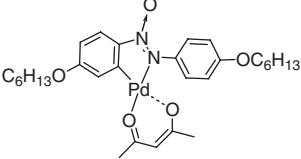
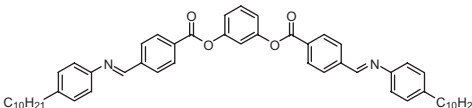
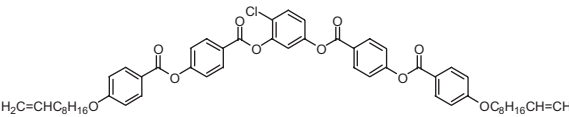
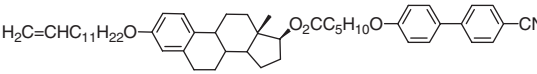
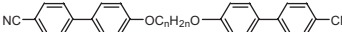
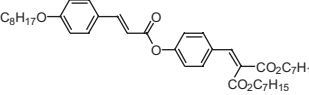
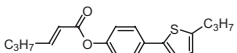
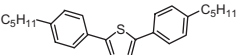
The flexoelectric effect was measured initially using 4-methylbenzylidene-4'-butylaniline (MBBA), whose structure is shown as compound (**1**), see Table 1. MBBA has rigid rod-like molecular structure and is generally regarded as a standard calamitic liquid crystal with a non-polar nematic phase at room temperature (13). Several bistable nematic prototypes (8, 12) were demonstrated using homologues of the calamitic 4-*n*-alkyl-4'-cyanobiphenyl nematic liquid crystals, such as 4-cyano-4'-pentylbiphenyl (K15) and 4-cyano-4'-heptyloxybiphenyl (**2**), synthesised over thirty years ago. Surprisingly only a few nematic and chiral nematic liquid crystals, such as the compounds (**3–10**) shown in Table 1, have been synthesised specifically to study the flexoelectric properties of their nematic phases (14–23). The values of the flexoelectric coefficient of the nematic phase required for use in individual types of LCD is either not known or is commercially sensitive information. It is self-evident that high values of the flexoelectric coefficients will lead to shorter response times and/or lower operating voltages.

The flexoelectric coefficients of nematic mixtures of the organometallic dopant (**3**) with a clearly non-linear or rod-like molecular shape and 4-methylbenzylidene-4'-butylaniline (MBBA) were found (14) to be similar to

those of the host nematic material itself (**1**) (13). The bent-core molecule (**4**), consisting of five phenyl rings connected by a mixture of ester and imine linking groups, as a dopant in a nematic mixture was reported to exhibit a large flexoelectric effect, e.g. the presence of a small amount (5 wt%) of this bent-core dopant was found to substantially increase (+30%) the flexoelectric coefficients ($e_s + e_b/\kappa$) of the host mixture (E7) as well as changing the sign of the combined flexoelectric coefficients (15). Much more recently a large banana-shaped or bent-core compound (**5**) consisting of five phenyl rings connected by four ester linking units was reported to exhibit a giant flexoelectric effect due to its bent shape and a large dipole moment (16). Unfortunately, very large bent-core compounds may not be suitable as practical dopants in commercial flexoelectric nematic mixtures, or as the major or only components in nematic mixtures, as they are very viscous and consequently may induce very high operating voltages and/or slow response times in LCDs in spite of large flexoelectric effects.

A diverse series of liquid crystalline dimers consisting of substituted aromatic molecular cores connected by an aliphatic spacer induce a large flexoelectric effect as dopants in nematic host mixtures or as nematic mixtures made up only of themselves (8, 17–20). Such liquid crystalline dimers with an uneven number of methylene units (CH₂) in the aliphatic spacer can be assumed to adopt a banana-shaped conformation. This may also be the case for dimers with an even number of spacer units in the aliphatic chain, which can induce a significantly higher value of the flexoelectric coefficients than the same concentration of similar dimers with an uneven number of methylene units (CH₂) in the aliphatic spacer. (8, 17–20) These apparently linear dimers may also adopt a banana-shaped conformation due to molecular rotation about one of the carbon-carbon bonds between the methylene units. The flexoelectric coefficients of the chiral nematic liquid crystal bimesogenic compound (**6**), based on estradiol as chiral unit and highly polarisable cyanobiphenyl as

Table 1. Molecular structures, the flexoelectric ratio (\bar{e}/κ) and the average flexoelectric coefficient (\bar{e}) of the compounds (1–10) measured in different ways, see the table notes A–K. The corresponding values for the nematic mixture E7 are given for comparison purposes. The sign of the flexoelectric coefficients reported in the literature is not always given and is not always defined in the same way or using identical conventions (1–6).

Compound	\bar{e}/κ (C N ⁻¹ m ⁻¹)	\bar{e} (10 ⁻¹² C m ⁻¹)	Note
Nematic mixture E7	0.76–1.0		A
1 	1.0	1.5	B
2 	0.5		C
3 		1.8	D
4 	1.3		E
5 		62,000	F
6 	0.5		G
7 	0.6		H
8 		2.16	I
9 	0.12		J
10 	1.44		K

A measured using the nematic mixture E7 at room temperature using the HAN method (22). B measured using pure MBBA (1) at room temperature (13). C measured for a chiral nematic mixture of 4-cyano-4'-heptyloxybiphenyl (2) and a chiral dopant (4–6 wt%) above the melting point of the mixture (Cr–N* = 55°C) using the ULH method (8). D measured for a nematic mixture of the organometallic compound (3) (9 wt%) in MBBA at room temperature using the domain wall method (using $\bar{e}/\kappa = 1.3$ C m⁻¹ for MBBA) (14). E measured for a nematic mixture of 5 wt% of the five-ring compound (4) in E7 at room temperature using the ULH method (using $\bar{e}/\kappa = 1.0$ C m⁻¹ for E7) (15). F measured using a new method based on measuring the electric current produced by periodic mechanical flexing of the monotropic nematic phase of the pure five-ring tetra-ester (5) at 70°C (16). G measured above the melting point (Cr–N* = 68°C) of the pure asymmetrical estradiol dimer (6) using the ULH method (17, 18). H measured for a chiral nematic mixture of symmetrical cyano-biphenyl dimer (7) and a chiral dopant (4–6 wt%) above the melting point (Cr–N* = 175°C) of the mixture using the ULH method (19). I extrapolated to 100% from nematic mixtures of the swallow-tail compound (8) in 4-butyl-4'-methoxyazobenzene (BMOAB) at 29°C using the domain wall method (using $\bar{e} = 2.16 \times 10^{-12}$ C N⁻¹ m⁻¹ for BMAOB) (3, 4). J measured using pure two-ring 2,5-disubstituted thiophene (9) at room temperature using the HAN method (21). K measured for a nematic mixture of the three-ring 2,5-disubstituted thiophene (10) (10 wt%) in E7 at room temperature using the HAN method (using $\bar{e} = 0.76$ C N⁻¹ m⁻¹ for E7) (22).

the terminal group and several other mesogenic units, were measured in the pure state (17). However, the flexoelectric coefficients had to be measured at elevated temperatures due to the high melting points of the chiral nematic mixtures containing them (17). The nematic phase of the liquid crystalline dimers (7) were doped with chiral dopants to produce chiral nematic mixtures, whose flexoelectric coefficients were also measured (8, 18). The broad class of compounds represented by compounds (6) and (7) were designed for use in the ULH-LCD based on the flexoelectric effect in the chiral nematic phase and represent the best materials designed so far for this particular application (18). Mixtures of related polyfluorinated dimers have also been studied recently as flexoelectric nematic materials, and somewhat higher values for the flexoelectric coefficients have been determined (19, 20).

The flexoelectric properties of nematic mixtures of the swallow-tail compound (8) were investigated due to its pear-drop shape (3, 4). However, the induced values of the flexoelectric coefficients were small, perhaps due to the weak flexoelectric properties of the nematic host. Nematic liquid crystals with a banana shape, such as the 2,5-disubstituted thiophenes (9) and (10), were reported to exhibit small-to-relatively-large flexoelectric coefficients in either the pure state or as dopants in E7 at room temperature (21–23). The requirement for molecules with a banana shape appears to be confirmed by studies of the photo-induced *cis*- and *trans*-isomers of azo compounds (24). However, there are indications that linear molecules with a rigid rod-like aromatic core of limited shape anisotropy may also be useful dopants to induce large values of the flexoelectric coefficients (22). However, the liquid crystalline dopants studied were exclusively almost completely apolar or possessed a significant dipole moment across the long molecular axis.

Therefore, we now report the synthesis and characterisation of a series of linear molecules with a rod-like shape with limited shape anisotropy to be used as dopants for nematic mixtures to study the dependence of the flexoelectric coefficients on molecular structure in general and on the magnitude of a dipole moment parallel or orthogonal to the long molecular axis in particular. The materials synthesised are designed as dopants because the nematic phases of the pure materials would exhibit a very high viscosity. This would induce very long switching times in devices using them, as would most of the compounds listed in Table 1, which were also mostly measured as dopants in host nematic mixtures. The melting points of such materials are also too high to allow useful measurements of the flexoelectric coefficients of their nematic phase in the pure state to be made. MBBA is an exception; see Table 1. Two series of dopants of similar shape and chemical constitution, including many constitutional

isomers, have been prepared: one with a dipole moment across the long molecular axis, and a complementary series with a dipole moment essentially parallel to the long molecular axis. These compounds were chosen in part for the absence of molecular conformers, apart from that of the alkyl chain in a terminal position, which is the same for each compound studied; the use of accurate molecular models would be required for an unambiguous interpretation of the results, as the flexoelectric effect appears to depend on molecular shape.

Such dopants should satisfy a clear requirement for dopants for guest–host nematic mixtures to induce flexoelectric properties, rather than preparing nematic mixtures consisting only or mainly of flexoelectric components. The dopants should exhibit a spectrum of physical properties, i.e. they should be electrochemically, photochemically and thermally stable; they should be sufficiently soluble in the nematic host to induce the desired magnitude of the flexoelectric coefficients; ideally they should exhibit a low melting point and a high nematic–isotropic transition temperature; they should induce a low viscosity and a high value of the flexoelastic ratio (\bar{e}/κ), where $\bar{e} = (e_1 + e_3)/2$ is the average flexoelectric coefficient and $\kappa = (k_1 + k_3)/2$ is the average elastic constant, where k_1 and k_3 are the splay and bend elastic constants, respectively. The presence of dopants in nematic guest–host mixtures at such relatively low concentrations can induce large increases in the flexoelastic ratio (\bar{e}/κ) of such mixtures (15, 22, 23).

Theoretical models have been developed to correlate molecular structure to the flexoelectric effect (25–34). Unfortunately, although these theories have been improved steadily since the initial discovery of flexoelectricity, and become much more reliable over time, these models are not particularly helpful in the design of new liquid crystals with nematic phases with large flexoelectric coefficients. They differ significantly in the relative emphasis they place on the importance of shape anisotropy as well as dipolar and quadrupolar effects, although a recent mean-field model is remarkably successful in relating the dipolar and quadrupolar contributions to the flexoelectric response to molecular structure (25). Fortunately, there is now a range of reliable methods for measuring the flexoelectric coefficients to test and then hopefully validate one or more of these theories (35–43). For example, the uniformly lying helix (ULH) configuration is a relatively simple and reliable method for screening new compounds in chiral nematic mixtures for their efficacy in improving the flexoelectric response (5–8). We have chosen to use this method to evaluate the flexoelectric properties of nematic mixtures containing the new materials for these reasons (5–8).

In addition, the results of the investigation of doped nematic mixtures containing the same or very similar dopants should allow comparison of the magnitude of the flexoelectric coefficients of the nematic guest–host mixtures determined by different methods, i.e. the HAN and UHL methods. These methods use the deformation of nematic domains, the use of ULH-LCD cells and HAN cells, AC and DC methods as well as leaky wave-guide methods. Similar relative values are found using different methods, although the absolute values can vary by a factor of two or more; see Table 1. However, exact comparisons are often difficult to make, because the reported measurements often use different methods of determination at different absolute or reduced temperatures using amounts (wt% or mol%) of the compounds to be investigated in different nematic or chiral nematic hosts in different types of cells (see Table 1). Sometimes the magnitude of individual flexoelectric coefficients is given, sometimes the average value of e_1 and e_3 is reported, the sign of the flexoelectric coefficients is often unclear or disputed and sometimes the value quoted is divided by the average elastic constant, κ , which is often assumed not to change on addition of the dopant to be measured.

2. Experimental

2.1 Instrumentation

All commercially available starting materials, reagents and solvents were used as supplied from Aldrich, Strem Chem. Inc., Acros Lancaster Synthesis or Merck Technical Centre in Chilworth. All the reactions were carried out under a dry nitrogen atmosphere and the temperature was measured internally. Mass spectra were determined using a Gas Chromatography/Mass Spectrometer (GC/MS)-QP5050A Shimadzu with Electron Impact (EI) at a source temperature of 200°C and the mass ion of the material is given as M^+ . ^1H NMR spectra were recorded using a JEOL Lambda 400 spectrometer with tetramethylsilane (TMS) as an internal standard. Purification of the reaction intermediates and final products was achieved by column chromatography, using silica gel (40–63 μm , 60 Å) obtained from Fluorochem, and recrystallisation from appropriate organic solvents. The melting point and other liquid crystal transition temperatures were measured using a Linkam 350 hot-stage and control unit in conjunction with a Nikon E400 polarising microscope. The liquid crystal transition temperatures of the final products and those of the guest–host nematic mixtures containing them as dopants were also determined using a Perkin-Elmer DSC-7 and in conjunction with a TAC 7/3 instrument controller. The peak value of the transition is reported. The purity of the final compounds was

determined by elemental analysis using a Chromopack CP3800 gas chromatograph equipped with a 10 m CP-SIL 5CB column. AM1 calculations were carried out using ChemDraw pro 3D MOPAC 2000. The physical property data given in Tables 2 and 3 were measured on instruments at the Merck Technical Centre in Chilworth using standard techniques. The dielectric permittivity and elastic constants were measured using the host nematic mixture MLC-6437-000 doped with 8 wt% of the test materials as dopants. The flexoelectric ratio was then determined using the same guest–host nematic mixtures with the addition of a small amount (1.8 wt%) of the standard Merck chiral dopant A to the mixtures in order to produce a chiral nematic phase required for measurement of flexoelectric coefficients using the UHL method (5–8).

2.2 Synthesis

A series of Suzuki aryl–aryl coupling reactions (44–47) between aryl halides and triflates with aryl boronic acids, see Scheme 1 for a typical reaction, were used to synthesise the compounds (11–29) collated in Tables 1 and 4. The phenyl and biphenyl boronic acids were either commercially available or prepared by conversion of phenyl and biphenyl halides into the corresponding phenyl boronic acids using standard procedures (44–47). The required phenyl and biphenyl triflates were produced from the corresponding phenols in a standard way; see Scheme 1 (48). The 2,3-difluoro-4,4''-dipentyl-*p*-terphenyl (14) (49) and the 4-cyano-4''-pentyl-*p*-terphenyl (22) (50) were supplied by the E. Merck Chilworth Technical Centre, Southampton, UK. The reference 4,4''-dipentyl-*p*-terphenyl (11) (51), the substituted 4,4''-dipentyl-*p*-terphenyls (12, 13 and 15) (52, 53), the 2,5-disubstituted pyridine (16) (54) and 2,5-disubstituted pyrimidine (17) (55) are shown in Table 1. The 2,5-disubstituted pyridazine (18) (56) was available from a previous programme (22). The substituted 4-pentyl-*p*-terphenyls (19–21 and 23–29) (57, 58) synthesised using these methods are listed in Table 4.

2.2.1 4-Pentylphenylboronic acid

A solution of *n*-butyl lithium in hexane (21.10 cm^3 , 2.5 M, 52.80 mmol) was added drop wise to a stirred solution of 1-bromo-4-pentylbenzene (10.00 g, 43.50 mmol) in THF (250 cm^3) at -78°C and left to react (1 h). Trimethyl borate (13.60 g, 130 mmol) was then added drop wise over a period of 30 minutes at -78°C . The reaction mixture was stirred and allowed to warm to room temperature overnight. The reaction mixture was then stirred with 20% hydrochloric acid (300 cm^3) before being extracted with diethyl ether (2 \times 200 cm^3). The combined organic extracts were

Table 2. Molecular structures, dielectric constants (ϵ_{\parallel} and ϵ_{\perp}), dielectric anisotropy ($\Delta\epsilon$), splay and bend elastic constants (k_1 and k_3), flexoelectric ratio (\bar{e}/κ), average flexoelectric coefficient (\bar{e}) and nematic clearing point (T_{N-I}) of the guest-host nematic mixtures incorporating 8 wt% of the fluoro-substituted 4,4''-dialkyl-*p*-terphenyls (**12**, **13** and **30**), the 2,5-disubstituted pyridine (**16**) and the fluoro-substituted 4-pentyl-*p*-terphenyls (**21** and **23–26**) as dopants in the host mixture MLC-6437-000, whose values are also given for comparison purposes.

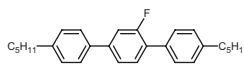
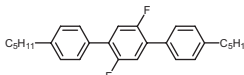
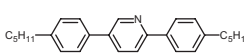
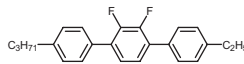
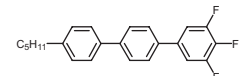
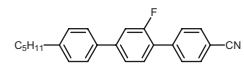
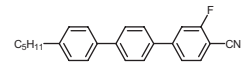
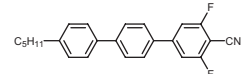
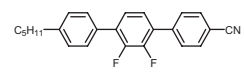
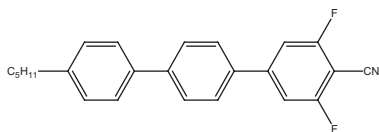
Compound	ϵ_{\parallel}	ϵ_{\perp}	$\Delta\epsilon$	k_1 (10^{-12} N)	k_3 (10^{-12} N)	\bar{e}/κ ($C\ m^{-1}\ N^{-1}$)	\bar{e} (10^{-12} C m^{-1})	T_{N-I} °C
MLC6437-000	25.55	7.45	18.1	8.33	10.33	0.34	3.2	67
12 	24.79	6.76	18.0	9.29	10.76	0.27	2.72	68
13 	24.69	6.71	17.9	9.31	10.99	0.27	2.72	68
16 	22.71	6.49	16.2	9.58	10.46	0.29	2.91	74
30 	23.52	6.84	16.7	9.16	10.99	0.25	2.54	66
21 	26.17	6.94	19.2	8.83	9.92	0.36	3.39	64
23 	24.68	6.76	17.9	8.48	9.03	0.35	3.10	66
24 	26.69	7.05	19.6	8.83	10.34	0.34	3.29	74
25 	28.37	7.44	20.9	8.32	9.74	0.41	3.68	67
26 	24.18	6.88	17.3	8.43	9.04	0.36	3.12	65

Table 3. The flexoelectric ratio (\bar{e}/κ) of guest–host nematic mixtures incorporating 8 wt% of the 4-cyano-3,5-difluoro-4''-pentyl-*p*-terphenyl (**25**) as a dopant in the test nematic mixture MLC-6437-000 and the commercial nematic mixtures E7 and ZLI-4792. The corresponding values for the host nematic mixtures are given for comparison purposes.

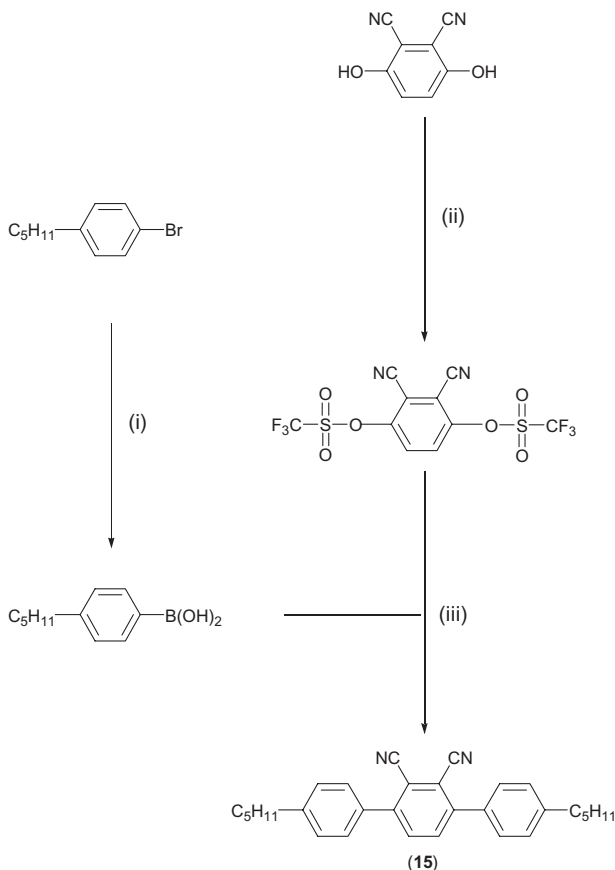


Dopant %	\bar{e}/κ in MLC-6437-000 ($C\ N^{-1}\ m^{-1}$)	\bar{e}/κ in E7 ($C\ N^{-1}\ m^{-1}$)	\bar{e}/κ in ZLI-4792 ($C\ N^{-1}\ m^{-1}$)
Pure host	0.34	0.38	0.16
2		0.40	0.17
4		0.43	0.19
8	0.41	0.50	0.21
16		0.62	0.26

washed with water ($2 \times 200\ cm^3$) and dried ($MgSO_4$). The solvent was removed under reduced pressure to yield a white solid (6.65g, 73%), which was used in the next step without further purification.

2.2.2 4,4''-Dipentyl-[1,1',4',1'']-terphenyl (11)

A mixture of *tetrakis*(triphenylphosphine)palladium (0) (0.24 g, 0.21 mmol), 4-pentylphenyl boronic acid (1.02 g, 5.30 mmol), 1,4-dibromobenzene (0.50 g, 2.11 mmol), aqueous 2 M sodium carbonate solution ($3.5\ cm^3$) and 1,2-dimethoxyethane ($30\ cm^3$) was heated under reflux overnight. The reaction mixture was allowed to cool to room temperature, poured into water and then the resultant mixture was extracted with diethyl ether ($3 \times 30\ cm^3$). The combined organic extracts were washed with brine ($3 \times 30\ cm^3$), dried ($MgSO_4$), evaporated down under reduced pressure and the residue was then purified by column chromatography using hexane as the eluent and recrystallisation from ethanol to yield a white solid (0.20 g, 41%). Cr–SmA = $192^\circ C$; SmA–I = $213^\circ C$. Cr–S = $192^\circ C$; S–I = $213^\circ C$ (51). $^1H\ NMR$ ($CDCl_3$) δ_H :



Scheme 1. Reagents and conditions: (i) (a) *n*-Butyllithium, THF, (-78°C); (b) $\text{B}(\text{OCH}_3)_3$; (c) $\text{HCl}(\text{aq})$, (ii) (a) Trifluoromethanesulphonic acid anhydride, DCM, (b) 2,6-lutidine (0°C); (c) H_2O , (iii) $(\text{PPh}_3)_4$, 2M Na_2CO_3 (aq), 1,2-dimethoxyethane (reflux).

0.91 (t, 6H, $J = 7.9$ Hz), 1.35 (sext, 4H), 1.37 (quint, 2H), 1.64 (quint, 4H), 2.65 (t, 4H, $J = 8.0$ Hz), 7.27 (d, 4H, 8.2 Hz), 7.56 (d, 4H, $J = 8.4$ Hz), 7.67 (d, 4H, $J = 9.0$ Hz). IR $\nu_{\text{max}}/\text{cm}^{-1}$: 2956, 2923, 2852, 1909, 1493, 1466, 1399, 1378, 1258, 1144, 1119, 1002, 827, 801, 754, 726. MS m/z : 370 (M^+ , M100), 313, 256. Combustion Analysis: Calculated: C (90.75%), H (9.25%). Found: C (90.77%), H (9.00%). GC/MS: 100%, M^+ . HPLC: 98.9%.

2.2.3 2'-Fluoro-4, 4''-dipentyl-[1,1',4',1'']-terphenyl (12)

A mixture of *tetrakis*(triphenylphosphine)palladium (0) (0.76 g, 0.66 mmol), 4-pentylphenyl boronic acid (3.15 g, 16.40 mmol), 4-bromo-2-fluoro-1-iodobenzene (2.00 g, 6.58 mmol), aqueous 2M sodium carbonate solution (10.0 cm^3) and 1, 2-dimethoxyethane (30 cm^3) was heated under reflux overnight. The solution was allowed to cool to room temperature, poured into water and the resultant mixture then extracted with

diethyl ether (3 \times 30 cm^3). The combined organic extracts were washed with brine (3 \times 30 cm^3), dried (MgSO_4), evaporated down under reduced pressure and the residue then purified by column chromatography using hexane as the eluent and recrystallisation from ethanol to yield a white solid (1.75 g, 71%). Cr–SmB = 51°C ; SmB–SmA = 62°C ; SmA–N = 109°C ; N–I = 137°C . Cr–SmB = 52°C ; SmB–SmA = 62°C ; SmA–N = 110°C ; N–I = 137°C (52). ^1H NMR (CDCl_3) δ_{H} : 0.91 (t, 3H, $J = 6.76$ Hz), 1.33 (sext, 2H), 1.35 (quint, 2H), 1.65 (quint, 2H), 2.65 (t, 2H, $J = 7.8$ Hz), 7.27 (d, 4H, $J = 7.8$ Hz), 7.37 (dd, 1H), 7.42 (dd, 1H), 7.49 (dd, 1H), 7.54 (d, 4H, $J = 8.16$ Hz). IR $\nu_{\text{max}}/\text{cm}^{-1}$: 2953, 2926, 2854, 1618, 1577, 1546, 1488, 1397, 1302, 1259, 1182, 1133, 1016, 1006, 893, 852, 733. MS m/z : 388 (M^+), 331 (M100), 274. Combustion Analysis: Calculated: C (86.55%), H (8.56%). Found: C (86.45%), H (8.82%). GC/MS: 100%, M^+ . HPLC: 98.8%.

2.2.4 2',5'-Difluoro-4,4''-dipentyl-[1,1',4',1'']-terphenyl (13)

A mixture of *tetrakis*(triphenylphosphine)palladium (0) (0.42 g, 0.37 mmol), 4-pentylphenyl boronic acid (1.76 g, 9.18 mmol), 1,4-dibromo-2,5-difluorobenzene (1.00 g, 3.66 mmol), aqueous 2M sodium carbonate solution (8.0 cm^3) and 1,2-dimethoxyethane (30 cm^3) was heated under reflux overnight. The solution was allowed to cool to room temperature, poured into water and the resultant mixture then extracted with diethyl ether (3 \times 30 cm^3). The combined organic extracts were washed with brine (3 \times 30 cm^3), dried (MgSO_4), evaporated down under reduced pressure and then purified by column chromatography using hexane as the eluent and recrystallisation from ethanol to yield a white solid (0.85 g, 57%). Cr–N = 63°C ; N–I = 85°C . ^1H NMR (CDCl_3) δ_{H} : 0.91 (t, 3H, $J = 7.0$ Hz), 1.33 (sext, 2H), 1.37 (quint, 2H), 1.65 (quint, 2H), 2.66 (t, 2H, $J = 7.8$ Hz), 7.24 (t, 2H, $J = 9.0$ Hz), 7.29 (d, 4H, $J = 8.4$ Hz), 7.50 (d, 4H, $J = 8.16$ Hz). IR $\nu_{\text{max}}/\text{cm}^{-1}$: 2927, 2858, 1914, 1612, 1529, 1486, 1394, 1268, 1170, 1123, 1018, 885, 844, 792. MS m/z : 406 (M^+), 349 (M100), 292. Combustion Analysis: Calculated: C (82.72%), H (7.93%). Found: C (82.28%), H (8.13%). GC/MS: 100%, M^+ . HPLC: 99.3%.

2.2.5 2,3-Dicyano-4-trifluoromethane-sulphonyloxyphenyl ester

A solution of trifluoromethane sulphonic acid anhydride (17.63 g, 62.5 mmol) in DCM (100 cm^3) was added to a stirred mixture of 3,6-dihydroxyphthalonitrile (2 g, 12.50 mmol) and 2,6-lutidine (6.69 g 62.5 mmol) in DCM (50 cm^3) at 0°C . The temperature of the

Table 4. Molecular structure and liquid crystal transition temperatures of the substituted 4,4''-dipentyl-*p*-terphenyls (**11–15**), 2,5-disubstituted pyridine (**16**), pyrimidine (**17**), pyridazine (**18**) and the substituted 4-pentyl-*p*-terphenyls (**19–29**).

	Structure	Cr		SmB		SmA		N		I
11		•	192	–	•	213	–	•		•
12		•	51	•	62	•	109	•	137	•
13		•	63	–	–	–	•	85	•	•
14		•	60	–	–	–	•	120	•	•
15		•	152	–	–	–	–	–	–	•
16		•	99	–	•	205	–	–	–	•
17		•	106	–	•	195	–	–	–	•
18		•	194	–	•	226	•	227	•	•
19		•	207	–	–	–	–	–	–	•
20		•	80	–	•	128	•	147	•	•
21		•	94	–	–	–	•	97	•	•
22		•	130	–	–	–	•	239	•	•
23		•	82	–	–	–	•	143	•	•
24		•	86	–	–	–	•	183	•	•
25		•	103	–	–	–	•	120	•	•
26		•	101	–	•	170	•	175	•	•
27		•	91	–	–	–	•	122	•	•
28		•	27	–	–	–	•	45	•	•
29		•	96	–	–	–	–	–	–	•

reaction mixture was allowed to rise to room temperature, stirred for 5 h, then the reaction mixture was added to water (200 cm³) and the product extracted into DCM (3 × 50 cm³). The combined organic layers were washed

with a 10% aqueous sodium carbonate solution (2 × 100 cm³), dried (MgSO₄), filtered and the filtrate evaporated down. The crude product was purified by column chromatography using hexane and ethyl acetate (80:20) as

eluent and recrystallisation from ethanol to yield (2.75 g, 52%) of the desired product. M.p. 127°C. $^1\text{H NMR}$ (CDCl_3) δ_{H} : 7.90 (d, 2H). IR $\nu_{\text{max}}/\text{cm}^{-1}$: 1472, 1435, 1208, 1128, 954, 839, 810. MS m/z : 424 (M^+), 227 (M100). Combustion Analysis: Calculated: C (28.30%), H (0.47%), N (6.60%), S (15.09%). Found: C (28.55%), H (0.54%), N (6.42%), S (15.27%).

2.2.6 4,4''-Dipentyl-[1,1',4',1'']-terphenyl-2',3'-dicarbonitrile (15)

A mixture of tetrakis(triphenylphosphine)palladium (0) (0.14 g, 0.12 mmol) and 4-pentylphenyl boronic acid (0.91 g, 4.72 mmol), 2,3-dicyano-benzene-1,4-disulphonic acid ditrifluoromethyl ester (0.50 g, 1.80 mmol), aqueous 2 M sodium carbonate solution (10 cm^3), water and 1,2-dimethoxyethane (30 cm^3) was heated under reflux overnight. The solution was allowed to cool to room temperature, poured into water and the resultant mixture then extracted into diethyl ether (3 \times 50 cm^3). The combined organic extracts were then washed with brine (3 \times 50 cm^3), dried (MgSO_4), evaporated down under reduced pressure and the residue then purified by column chromatography using hexane and ethyl acetate (80:20) as the eluent and recrystallisation from ethanol to yield a white solid (0.24 g, 48%). M.p. 152°C. $^1\text{H NMR}$ (CDCl_3) δ_{H} : 0.91 (t, 3H, $J = 7.0$ Hz), 1.33 (sext, 2H), 1.37 (quint, 2H), 1.65 (quint, 2H), 2.66 (t, 2H, $J = 7.8$ Hz), 7.24 (t, 2H, $J = 9.0$ Hz), 7.35 (d, 4H, $J = 8.16$ Hz), 7.51 (d, 4H, $J = 8.16$ Hz), 7.76 (s, 2H). IR $\nu_{\text{max}}/\text{cm}^{-1}$: 2229, 2845, 2230, 1610, 1520, 1467, 1121, 1015, 855, 901. MS m/z : 420 (M^+), 363 (M100), 306. Combustion Analysis: Calculated: C (85.67%), H (7.67%), N (6.66%). Found: C (85.92%), H (7.90%), N (6.72%).

2.2.7 2,5-Bis-(4-pentylphenyl)pyridine (16)

A mixture of tetrakis(triphenylphosphine)palladium (0) (0.11 g, 0.99 mmol), 4-pentylphenyl boronic acid (0.37 g, 1.97 mmol), 2,5-dibromopyridine (0.3 g, 0.99 mmol), aqueous 2 M sodium carbonate solution (10 cm^3), water and 1,2-dimethoxyethane (30 cm^3) was heated under reflux overnight. The solution was allowed to cool to room temperature, poured into water and the resultant mixture then extracted into diethyl ether (3 \times 50 cm^3). The combined organic extracts were then washed with brine (3 \times 50 cm^3), dried (MgSO_4), evaporated down under reduced pressure and purified by column chromatography using hexane and ethyl acetate (95:5) as the eluent and recrystallisation from ethanol to yield a white solid (1.89 g, 36%). Cr-SmA = 105°C; SmA-I = 206°C. Cr-S = 99°C; S-I = 205°C (54). $^1\text{H NMR}$ (CDCl_3) δ_{H} : 0.91 (t, 6H, $J = 6.76$ Hz), 1.36 (sext, 4H),

1.38 (quint, 4H), 1.66 (quint, 4H), 2.65 (t, 4H, $J = 7.88$ Hz), 7.29 (d, 4H, $J = 8.12$ Hz), 7.78 (d, 2H, $J = 8.16$ Hz), 7.94 (d, 2H, $J = 8.16$ Hz), 7.94 (d, 2H, $J = 8.12$ Hz), 8.91 (s, 1H). IR $\nu_{\text{max}}/\text{cm}^{-1}$: 2923, 2853, 1590, 1474, 1013, 998. MS m/z : 371 (M^+), 314 (M100), 257. Combustion Analysis: Calculated: C (90.75%), H (9.25%). Found: C (90.77%), H (9.00%). GC/MS: 100%, M^+ . HPLC: 98.1%.

2.2.8 2,5-Bis-(4-pentylphenyl)pyrimidine (17)

A mixture of tetrakis(triphenylphosphine)palladium (0) (0.60 g, 0.53 mmol) and 4-pentylphenyl boronic acid (3.03 g, 15.79 mmol), 5-bromo-2-iodo-pyrimidine (1.5 g, 5.27 mmol), aqueous 2 M sodium carbonate solution (10 cm^3), water and 1,2-dimethoxyethane (60 cm^3) was heated under reflux overnight. The solution was allowed to cool to room temperature, poured into water and the resultant mixture then extracted into diethyl ether (3 \times 50 cm^3). The combined organic extracts were washed with brine (3 \times 50 cm^3), dried (MgSO_4), evaporated down under reduced pressure and purified by column chromatography using hexane and ethyl acetate (90:10) as the eluent and recrystallisation from ethanol to yield a white solid (1.04 g, 53%). Cr-SmA = 106°C; SmA-I = 195°C. Cr-SmA = 106°C; SmA-I = 195°C (55). $^1\text{H NMR}$ (CDCl_3) δ_{H} : 0.90 (t, 6H, $J = 6.76$ Hz), 1.35 (sext, 4H), 1.38 (quint, 4H), 1.66 (quint, 4H), 2.68 (t, 4H, $J = 7.56$ Hz), 7.32 (d, 2H, $J = 5.64$ Hz), 7.34 (d, 2H, $J = 5.60$ Hz), 7.54 (d, 2H, $J = 8.16$ Hz), 8.37 (d, 2H, $J = 8.44$ Hz), 8.96 (s, 2H). IR $\nu_{\text{max}}/\text{cm}^{-1}$: 3031, 2920, 2853, 1610, 1578, 1378, 1116, 1015, 964. MS m/z : 372 (M^+), 315 (M100), 258. Combustion Analysis: Calculated: C (83.87%), H (8.60%), N (7.52%). Found: C (83.96%), H (8.90%), N (7.54%).

2.2.9 4-Fluoro-4''-pentyl-[1,1',4',1'']-terphenyl (19)

A mixture of tetrakis(triphenylphosphine)palladium (0) (0.23 g, 0.20 mmol), 4-pentylphenyl boronic acid (0.42 g, 2.19 mmol), 4-bromo-4'-fluorobiphenyl (0.50 g, 1.99 mmol), aqueous 2 M sodium carbonate solution (3.6 cm^3) and 1,2-dimethoxyethane (30 cm^3) was heated under reflux overnight. The solution was allowed to cool to room temperature and then poured into water and the resultant mixture then extracted with diethyl ether (3 \times 30 cm^3). The combined organic extracts washed with brine (3 \times 30 cm^3), dried (MgSO_4), evaporated down under reduced pressure and the residue purified by column chromatography using hexane as the eluent and recrystallisation from ethanol to yield a white solid (0.30 g, 50%). M.p. 207°C. $^1\text{H NMR}$ (CDCl_3) δ_{H} : 0.91 (t, 3H, $J = 6.76$ Hz), 1.30 (sext, 2H), 1.35 (quint, 2H), 1.65 (quint, 2H),

2.65 (t, 2H, $J = 7.60$ Hz), 7.16 (t, 2H, $J = 8.72$ Hz), 7.28 (d, 2H, $J = 8.4$ Hz), 7.56 (d, 2H, $J = 8.4$ Hz), 7.62 (d, 2H, $J = 6.72$ Hz), 7.64 (d, 2H, $J = 6.5$ Hz), 7.68 (d, 2H, $J = 8.44$ Hz). IR $\nu_{\max}/\text{cm}^{-1}$: 2929, 2856, 1602, 1492, 1466, 1396, 1215, 1224, 1161, 1102, 1002, 816, 743, 725, 648. MS m/z : 318 (M^+), 261 (M100), 119, 131, 165. Combustion Analysis: Calculated: C (86.75%), H (7.28%). Found: C (86.65%), H (7.45%). GC/MS: 100%, M^+ . HPLC: 100%.

2.2.10 2'',4''-Difluoro-4-pentyl-[1,1',4',1'']-terphenyl (20)

A mixture of *tetrakis*(triphenylphosphine)palladium (0) (0.30 g, 0.52 mmol), 4-pentylbiphenyl-4'-yl boronic acid (0.76 g, 2.48 mmol), 4-bromo-1,3-difluorobenzene (0.50 g, 2.59 mmol), aqueous 2 M sodium carbonate solution (4.0 cm^3), water and 1,2-dimethoxyethane (30 cm^3) was heated under reflux overnight. The solution was allowed to cool to room temperature, poured into water and the resultant mixture then extracted into diethyl ether (3 \times 30 cm^3). The combined organic extracts were washed with brine (3 \times 30 cm^3), dried (MgSO_4), evaporated down under reduced pressure and then purified by column chromatography using hexane as the eluent and recrystallisation from ethanol to yield a white solid (0.4 g, 46.0%). Cr–SmA = 80°C; SmA–N = 128°C; N–I = 147°C. ^1H NMR (CDCl_3) δ_{H} : 0.91 (t, 3H, $J = 6.76$ Hz), 1.33 (sext, 2H), 1.35 (quint, 2H), 1.65 (quint, 2H), 2.65 (t, 2H, $J = 7.8$ Hz), 6.92 (td, 1H), 6.98 (td, 1H), 7.27 (d, 2H, $J = 7.8$ Hz), 7.45 (dd, 1H), 7.56 (d, 4H, $J = 9.0$ Hz), 7.68 (d, 2H, $J = 8.6$ Hz). IR $\nu_{\max}/\text{cm}^{-1}$: 2927, 2854, 1618, 1597, 1533, 1490, 1434, 1396, 1270, 1142, 1101, 1005, 965, 849, 834, 804, 733. MS m/z : 336 (M^+), 279 (M100), 257. Combustion Analysis: Calculated: C (82.11%), H (6.59%). Found: C (81.88%), H (6.75%). GC/MS: 100%, M^+ . HPLC: 96.3%.

2.2.11 4-Pentyl-3'',4'',5''-trifluoro-[1,1',4',1'']-terphenyl (21)

A mixture of *tetrakis*(triphenylphosphine)palladium (0) (0.19 g, 0.17 mmol) and 4-pentylbiphenyl-4'-yl boronic acid (0.319 g, 1.81 mmol), 5-bromo-1,2,3-trifluorobenzene (0.50 g, 1.65 mmol), aqueous 2 M sodium carbonate solution (2.5 cm^3), water and 1,2-dimethoxyethane (30 cm^3) was heated under reflux overnight. The solution was allowed to cool to room temperature, poured into water and the resultant mixture then extracted into diethyl ether (3 \times 30 cm^3). The combined organic extracts were washed with brine (3 \times 30 cm^3), dried (MgSO_4), evaporated down under

reduced pressure and then purified by column chromatography using hexane as the eluent and recrystallisation from ethanol to yield a white solid (0.38 g, 65%). Cr–N = 94°C; N–I = 97°C. ^1H NMR (CDCl_3) δ_{H} : 0.91 (t, 3H, $J = 7.0$ Hz), 1.32 (sext, 2H), 1.38 (quint, 2H), 1.65 (quint, 2H), 2.67 (t, 2H, 7.6 Hz), 7.28 (d, 2H, $J = 6.5$ Hz), 7.31 (d, 2H, $J = 6.72$ Hz), 7.56 (d, 2H, $J = 8.44$ Hz), 7.59 (d, 2H, $J = 8.72$ Hz), 7.70 (d, 2H, $J = 8.72$ Hz). IR $\nu_{\max}/\text{cm}^{-1}$: 2961, 2932, 2861, 1913, 1615, 1542, 1496, 1443, 1398, 1366, 1255, 1129, 1045, 1002, 865, 808, 774, 706. MS m/z : 354 (M^+), 297 (M100), 149, 165. Combustion Analysis: Calculated: C (77.95%), H (5.97%). Found: C (77.73%), H (5.96%). GC/MS: 100%, M^+ . HPLC: 99.5%.

2.2.12 2'-Fluoro-4''-pentyl-[1,1',4',1'']-terphenyl-4-carbonitrile (23)

A mixture of *tetrakis*(triphenylphosphine)palladium (0) (0.84 g, 0.72 mmol), 4-pentylphenyl boronic acid (2.78 g, 14.48 mmol), 4'-bromo-2'-fluorobiphenyl-4-carbonitrile (2 g, 7.24 mmol), aqueous 2 M sodium carbonate solution (10 cm^3) and 1,2-dimethoxyethane (70 cm^3) was heated under reflux overnight. The solution was allowed to cool to room temperature, poured into water and the resultant mixture then extracted with diethyl ether (3 \times 50 cm^3). The combined organic extracts were then washed with brine (3 \times 50 cm^3), dried (MgSO_4), evaporated down under reduced pressure and the residue purified by column chromatography using hexane and ethyl acetate (80:20) as the eluent and recrystallisation from ethanol to yield a white solid (1.10 g, 46%). Cr–N = 82°C; N–I = 143°C. Cr–N = 82°C; N–I = 143°C (57,58). ^1H NMR (CDCl_3) δ_{H} : 0.91 (t, 3H, $J = 6.76$ Hz), 1.33 (sext, 2H), 1.36 (quint, 2H), 1.66 (quint, 2H), 2.65 (t, 2H, $J = 8.16$ Hz), 7.28 (d, 2H, $J = 8.16$ Hz), 7.43 (d, 1H, $J = 12.92$ Hz), 7.49 (d, 2H, $J = 8.16$ Hz), 7.54 (d, 2H, $J = 8.16$ Hz), 7.73 (d, 2H, $J = 8.16$ Hz), 7.75 (d, 2H, $J = 8.4$ Hz). IR $\nu_{\max}/\text{cm}^{-1}$: 2927, 2857, 2229, 1608, 1485, 1488, 1300, 1182, 1135, 878. MS m/z : 343 (M^+), 286 (M100), 165, 143. Combustion Analysis: Calculated: C (83.85%), H (6.40%), N (4.07%). Found: C (83.81%), H (6.66%), N (4.15%).

2.2.13 3''-Fluoro-4-pentyl-[1,1',4',1'']-terphenyl-4''-carbonitrile (24)

A mixture of *tetrakis*(triphenylphosphine)palladium (0) (1.34 g, 1.16 mmol) and 4-pentylbiphenyl-4'-yl boronic acid (3.74 g, 13.00 mmol), 4-bromo-2-fluoro-benzonitrile (2.50 g, 11.60 mmol), aqueous 2 M sodium carbonate solution (17.7 cm^3), water and 1,2-dimethoxyethane (30 cm^3) was heated under

reflux overnight. The solution was allowed to cool to room temperature, poured into water and the resultant mixture then extracted into diethyl ether ($3 \times 30 \text{ cm}^3$) and the combined organic extracts were then washed with brine ($3 \times 30 \text{ cm}^3$), dried (MgSO_4), evaporated down under reduced pressure and then purified by column chromatography using hexane as the eluent and recrystallisation from ethanol to yield a white solid (2.1 g, 54%). Cr–N = 86°C ; N–I = 183°C . Cr–N = 85°C ; N–I = 182°C . (57,58) $^1\text{H NMR}$ (CDCl_3) δ_{H} : 0.91 (t, 3H, $J = 6.76$ Hz), 1.33 (sext, 2H), 1.36 (quint, 2H), 1.66 (quint, 2H), 2.65 (t, 2H, $J = 7.56$ Hz), 7.29 (d, 2H, $J = 8.16$ Hz), 7.47 (dd, 1H), 7.53 (dd, 1H), 7.56 (dd, 1H), 7.65 (d 2H, $J = 8.4$ Hz), 7.72 (d, 2H, $J = 6.20$ Hz), 7.74 (d, 2H, $J = 8.12$ Hz). IR $\nu_{\text{max}}/\text{cm}^{-1}$: 2928, 2855, 2230, 1618, 1564, 1488, 1263, 1106, 1121, 901, 883, 812, 745. MS m/z : 343 (M^+), 286 ($\text{M}100$), 165, 143. Combustion Analysis: Calculated: C (83.93%), H (6.46%), N (4.08%). Found: C (83.71), H (6.71%), N (4.10%). GC/M: 100%, M ion. HPLC: 99.6%.

2.2.14 3'',5''-Difluoro-4-pentyl-[1,1',4',1'']-terphenyl-4''-carbonitrile (25)

A mixture of tetrakis(triphenylphosphine)palladium (0) (0.80 g, 0.696 mmol) and 4-pentylbiphenyl-4'-yl boronic acid (2.80 g, 10.0 mmol), 4-cyano-3,5-difluoro-benzenesulphonic acid trifluoromethyl ester (0.2g, 6.96 mmol), aqueous 2 M sodium carbonate solution (10 cm^3), water and 1,2-dimethoxyethane (50 cm^3) was heated under reflux overnight. The solution was allowed to cool to room temperature, poured into water and the resultant mixture then extracted into diethyl ether ($3 \times 30 \text{ cm}^3$). The combined organic extracts were washed with brine ($3 \times 30 \text{ cm}^3$), dried (MgSO_4), evaporated down under reduced pressure and then purified by column chromatography using hexane and ethyl acetate (90:10) as the eluent and recrystallisation from ethanol to yield a white solid (1.34 g, 53.4%). Cr–N = 103°C ; N–I = 120°C . Cr–N = 103°C ; N–I = 120°C (57,58). $^1\text{H NMR}$ (CDCl_3) δ_{H} : 0.91 (t, 3H, $J = 7.00$ Hz), 1.33 (sext, 2H), 1.36 (quint, 2H), 1.66 (quint, 2H), 2.65 (t, 2H, $J = 7.72$ Hz), 7.32 (t, 2H, $J = 8.72$ Hz), 7.55 (d, 2H, $J = 8.12$ Hz), 7.64 (d, 2H, $J = 8.44$ Hz), 7.73 (d, 4H, $J = 8.70$ Hz). IR $\nu_{\text{max}}/\text{cm}^{-1}$: 2928, 2855, 2230, 1618, 1564, 1488, 1263, 1106, 1121, 901, 883, 812, 745. MS m/z : 361 (M^+), 304 ($\text{M}100$). Combustion Analysis: Calculated: C (79.76%), H (5.86%), N (3.88%). Found: C (80.00%), H (6.12%), N (3.92%). GC/MS: 100%, M^+ . HPLC: 97.1%.

2.2.15 2',3'-Difluoro-4-pentyl-[1,1',4',1'']-terphenyl-4''-carbonitrile (26)

A mixture of tetrakis(triphenylphosphine)palladium (0) (0.57 g, 0.49 mmol) and 2,3-difluoro-4'-pentylbiphenyl-4-yl boronic acid (1.80 g, 5.93 mmol), 4-bromobenzenonitrile (0.90 g, 4.94 mmol), aqueous 2M sodium carbonate solution (10 cm^3), water and 1,2-dimethoxyethane (30 cm^3) was heated under reflux overnight. The solution was allowed to cool to room temperature, poured into water and the resultant mixture then extracted into diethyl ether ($3 \times 30 \text{ cm}^3$) and the combined organic extracts were then washed with brine ($3 \times 30 \text{ cm}^3$), dried (MgSO_4), evaporated under reduced pressure and then purified by column chromatography using hexane and ethyl acetate (90:10) as the eluent and recrystallisation from ethanol to yield a white solid (1.21 g, 68%). Cr–SmA = 101°C ; SmA–N = 170°C ; N–I = 175°C . $^1\text{H NMR}$ (CDCl_3) δ_{H} : 0.91 (t, 3H, $J = 6.76$ Hz), 1.34 (sext, 2H), 1.37 (quint, 2H), 1.66 (quint, 2H), 2.66 (t, 2H, $J = 7.88$ Hz), 7.24 (d, 2H, $J = 8.16$ Hz), 7.31 (d, 2H, $J = 8.40$ Hz), 7.51 (d, 2H, $J = 8.44$ Hz), 7.71 (d, 2H, $J = 8.68$ Hz), 7.77 (d, 2H, $J = 8.16$ Hz). IR $\nu_{\text{max}}/\text{cm}^{-1}$: 2921, 2855, 2236, 1610, 1525, 1483, 1202, 1099, 903, 849. MS m/z : 361 (M^+), 304 ($\text{M}100$), 282, 201. Combustion Analysis: Calculated: C (79.76%), H (5.86%), N (3.88%). Found: C (79.88%), H (6.01%), N (3.59%).

2.2.16 2',3',3''-Trifluoro-4-pentyl-[1,1',4',1'']-terphenyl-4''-carbonitrile (27)

A mixture of tetrakis(triphenylphosphine)palladium (0) (0.14 g, 0.13 mmol), 2,3-difluoro-4'-pentyl-biphenyl-4-yl-boronic acid (0.46 g, 1.50 mmol), to 4-bromo-3-fluorobenzenonitrile (0.25 g, 1.25 mmol), aqueous 2 M sodium carbonate solution (10 cm^3), water and 1,2-dimethoxyethane (30 cm^3) was heated under reflux overnight. The solution was allowed to cool to room temperature, poured into water and the resultant mixture then extracted into diethyl ether ($3 \times 50 \text{ cm}^3$). The combined extracts were then washed with brine ($3 \times 50 \text{ cm}^3$), dried (MgSO_4), evaporated down under reduced pressure and purified by column chromatography using hexane and ethyl acetate (90:10) as the eluent and recrystallisation from ethanol to yield a white solid (0.19 g, 40%). Cr–N = 91°C ; N–I = 122°C . $^1\text{H NMR}$ (CDCl_3) δ_{H} : 0.92 (t, 3H, $J = 6.76$ Hz), 1.35 (sext, 2H), 1.37 (quint, 2H), 1.67 (quint, 2H), 2.67 (t, 2H, $J = 7.60$ Hz), 7.23 (d, 2H, $J = 8.16$ Hz), 7.31 (d, 2H, $J = 8.12$ Hz), 7.37 (d, 2H, $J = 8.12$ Hz), 7.51 (d, 2H, $J = 8.44$ Hz), 7.73 (t, 1H, $J = 7.84$ Hz). IR $\nu_{\text{max}}/\text{cm}^{-1}$: 2922, 2851, 2237, 1621, 1566, 1483, 1402, 1102, 1120, 882, 817. MS m/z : 379(M^+), 322($\text{M}100$), 300, 282. Combustion Analysis: Calculated: C (75.98%), H

(5.27%), N (3.69%). Found: C (76.05%), H (5.28%), N (3.53%).

2.2.17 2',3',3'',5''-Tetrafluoro-4-pentyl-[1,1',4',1'']terphenyl-4''-carbonitrile (28)

A mixture of *tetrakis*(triphenylphosphine)palladium (0) (0.14 g, 0.12 mmol), 2,3-difluoro-4'-pentylbiphenyl-4-yl boronic acid (0.41 g, 1.34 mmol), 4-cyano-3,5-difluorophenyl-1-sulphonic acid trifluoromethyl ester (0.35 g, 1.22 mmol), aqueous 2 M sodium carbonate solution (10 cm³), water and 1,2-dimethoxyethane (30 cm³) was heated under reflux overnight. The solution was allowed to cool to room temperature, poured into water and the resultant mixture then extracted into diethyl ether (3 × 50 cm³). The combined organic extracts were then washed with brine (3 × 50 cm³), dried (MgSO₄), evaporated down under reduced pressure and the residue purified by column chromatography using hexane and ethyl acetate (90:10) as the eluent and recrystallisation from ethanol to yield a white solid (0.1 g, 21%). Cr–N = 27°C; N–I = 45°C. ¹H NMR (CDCl₃) δ_H: 0.91 (t, 3H, *J* = 6.74 Hz), 1.36 (sext, 2H), 1.37 (quint, 2H), 1.65 (quint, 2H), 2.67 (t, 2H, *J* = 7.60 Hz), 7.24 (d, 2H, *J* = 8.44), 7.31 (d, 4H, *J* = 8.44 Hz), 7.51 (d, 2H, *J* = 7.60 Hz). IR ν_{max}/cm⁻¹: 2926, 2853, 2239, 1623, 1562, 1482, 1102, 884, 816. MS *m/z*: 397(M⁺), 245(M100), 340, 202. Combustion Analysis: Calculated: C (72.53%), H (4.82%), N (3.52%). Found: C (72.61%), H (5.27%), N (3.39%).

2.2.18 2',3',3'',4'',5''-Pentafluoro-4-pentyl-[1,1';4',1'']-terphenyl (29)

A mixture of *tetrakis*(triphenylphosphine)palladium (0) (0.05 g, 0.05 mmol), 2,3-difluoro-4'-pentylbiphenyl-4-yl boronic acid (0.15 g 0.52 mmol), 5-bromo-1,2,3-trifluorobenzene (0.1 g, 0.47 mmol), aqueous 2 M sodium carbonate solution (10 cm³), water and 1,2-dimethoxyethane (30 cm³) was heated under reflux overnight. The solution was allowed to cool to room temperature, poured into water and the resultant mixture then extracted into diethyl ether (3 × 50 cm³). The combined organic extracts were then washed with brine (3 × 50 cm³), dried (MgSO₄), evaporated down under reduced pressure and purified by column chromatography using hexane as the eluent and recrystallisation from ethanol to yield a white solid (0.04 g, 22%). M.p. 96°C. ¹H NMR (CDCl₃) δ_H: 0.91 (t, 3H, *J* = 7.00 Hz), 1.35 (sext, 2H), 1.38 (quint, 2H), 1.66 (quint, 2H), 2.65 (t, 2H, *J* = 7.56 Hz), 7.19 (d, 2H, *J* = 7.4 Hz), 7.24 (d, H, *J* = 7.88 Hz), 7.29 (d, 2H, *J* = 8.44 Hz), 7.49 (d, 2H, *J* = 8.44 Hz). IR ν_{max}/cm⁻¹: 2929, 1617, 1533, 1489, 1461, 1424, 1249, 1102, 984, 892, 856.

MS *m/z*: 390(M⁺), 333(M100), 293. Combustion Analysis: Calculated: C (70.76%), H (4.91%). Found: C (70.49%), H (4.99%).

2.3 Mesomorphic properties

The mesomorphic behaviour and the liquid crystalline transition temperatures of the 4,4''-dipentyl-*p*-terphenyl (11), the substituted 4,4''-dipentyl-*p*-terphenyls (12–15), the nitrogen heterocycles (16–18) and the substituted 4-pentyl-*p*-terphenyls (19–29) shown in Table 4 as well as the nematic clearing point of the guest–host nematic mixtures containing them as dopants (8 wt%) were determined using polarising optical microscopy (POM). A nematic phase (N) was observed for all of the guest–host mixtures containing the compounds (11–29) as dopants and most of the individual compounds (11–29) in the pure state. A Schlieren texture with 2-brush and 4-brush disclinations is seen for the nematic phase between crossed polarisers in an optical microscope. Small droplets are seen on cooling slowly from the isotropic phase, which then coalesce to form the Schlieren texture of the nematic phase with two and four-point brushes. Several compounds (11, 12, 16–18, 20 and 26) exhibit a smectic A phase (SmA) on cooling the Schlieren texture of the nematic phase, or directly from the isotropic liquid, to form a focal conic texture as well as optically extinct areas in the same sample. Elliptical and hyperbolic lines of optical discontinuity typical of focal conic defects are also observed as usual. These textures are characteristic of the (uniaxial) SmA phase. Only compound (12) also exhibits a smectic B phase (SmB) on cooling from the SmA phase. Transition bars are seen on the backs of the focal conics at the transition from the SmA to the SmB phase on heating and cooling. The optically extinct areas present in the texture of the SmA phase remain in the SmB texture. This optical behaviour is consistent with the uniaxial nature of the SmB phase. The transition temperatures of the compounds (11–29) as well as those of the nematic mixtures containing them were observed first using optical microscopy and then confirmed by using Differential Scanning Calorimetry (DSC). The base line of the spectra was relatively flat in each case and sharp transition peaks are observed for the pure components (11–29) with no thermal degradation. Large melting transition peaks and transitions from the SmA and SmB phases to the nematic phase were observed. The peaks for the nematic–isotropic transition are relatively small, which is characteristic of a nematic phase. The nematic clearing point transitions for the nematic mixtures were much broader and less well defined as usual.

2.4 Physical properties

The flexoelastic ratio (\bar{e}/κ) was determined using the standard uniformly lying helix (ULH) procedure (5–8). The test nematic mixtures are made up of 8 wt% of each material to be tested dissolved in the host nematic mixture (MLC-6437-000). This permits an initial screening of the solubility of each material at a practically useful concentration for flexoelectric mixtures and allows comparisons of the physical properties of the doped mixtures to be made. The flexoelastic ratio and the splay and bend elastic constants (k_1 and k_3) listed in Table 2 were measured at a constant reduced temperature ($0.9 \times T_{N-I}$ in K) below the nematic clearing point of the mixture to facilitate comparison at the same reduced temperature. A chiral additive was used as a second dopant (1.8 wt%) in the test guest–host nematic mixture consisting of 8 wt% of each guest dopant dissolved in the host nematic mixture (MLC-6437-000). The presence of the chiral dopant was assumed to have little effect on the elastic, dielectric and flexoelectric properties of the nematic mixture. The pitch length, P_0 , of the doped chiral nematic mixtures was determined using the Cano-wedge technique at a constant reduced temperature ($0.9 \times T_{N-I}$ in K). The pitch was found to be about $0.5 \mu\text{m}$ with very little variation for the nematic host mixture and the guest–host mixtures shown in Table 2. The nematic mixtures exhibit a significant biphasic region consisting of co-existing nematic and isotropic regions. The clearing point quoted (T_{N-I}) in Table 2 is that measured half-way between the onset of the biphasic region and the complete disappearance of the nematic phase. The flexoelectric effect was determined in test glass cells with a $4.35 \mu\text{m}$ – $5 \mu\text{m}$ cell gap, rubbed polyimide alignment layers and transparent ITO electrodes on the inner walls of the cells. The samples were examined in a hot stage on a rotating sample stage of a polarising microscope (Olympus BX 51). Voltage wave forms were generated using a Wave Tek Arbitrary Wave form Generator 75 and the applied fields were varied in amplitude from zero to $15 \text{ V } \mu\text{m}^{-1}$. The flexoelectro-optic effect was observed with the chiral nematic helix perpendicular to both the applied field and the viewing direction, i.e. with the ULH form of the focal conic texture as well as the optic axis in the plane of the cell. The desired alignment was obtained by applying a low voltage across the cell, while unidirectionally shearing the cell, which promotes the uniform alignment of the disordered focal conic texture with the helical axis and the optic axis in the plane of the cell. The rotation angles of the optic axis, ϕ , were determined by placing the sample between crossed polarisers and measuring the half angle between the two positions of extinction. The

relationship between $\tan\phi$ and E is linear at low fields at the reduced temperature used. The rotation of optic axis through an angle, ϕ , induced by flexoelectric coupling (5–8) is related to the natural helical pitch of the phase as in the equation

$$\tan \phi = \bar{e}P_0E/2\pi\kappa$$

where $\bar{e} = (e_1 + e_3)/2$ is the average flexoelectric coefficient, P_0 is the pitch of the chiral nematic phase, E is the applied electric field and $\kappa = (k_1 + k_3)/2$ is the average elastic constant, where k_1 and k_3 are the splay and bend elastic constants, respectively. The error of measurement for the flexoelastic ratio (\bar{e}/κ) is estimated as 5–10%, taking into account errors from the gradient of ϕ versus E .

3. Results and discussion

3.1 Transition temperatures

The reference 4,4''-dipentyl-*p*-terphenyl (**11**) (51), the substituted 4,4''-dipentyl-*p*-terphenyls (**12–15**) (52, 53) and the nitrogen heterocycles (**16–18**) (54–56) collated in Table 4 are rigid and consist of three six-membered aromatic rings in a linear configuration with two pentyl chains in *para*-positions situated on the terminal phenyl rings (22, 49–58). This molecular structure is characterised by a high degree of symmetry and a limited degree of shape anisotropy. It is clear from the thermal data of the terphenyls (**11–15**) listed in Table 4 that the presence of lateral substituents, such as the fluorine atom, results in compounds with lower melting and clearing points, when compared with those of non-laterally substituted analogues, i.e. those with a hydrogen atom in place of the fluorine atom; for example, compare the transition temperatures of the fluoro-substituted terphenyls (**12–14**) with those of the reference 4,4''-dipentyl-*p*-terphenyl (**11**). The transition temperatures of the smectic phases are reduced, some smectic phases are eliminated in those compounds, e.g. compounds (**13** and **14**) with two fluorine atoms in a lateral position and a nematic phase is induced, i.e. the presence of one or more fluorine atoms in lateral positions disrupt the lamellar structure of smectic phases. The low transition temperatures are also due partly to directional steric effects increasing the intermolecular distance and thereby lowering the intermolecular forces of attraction and a higher degree of interannular twisting reducing the degree of molecular polarisability (57, 58).

The non-laterally substituted compounds (**11** and **16–18**) are similar in shape as are the laterally substituted terphenyls (**14** and **15**). The dinitrile (**15**) has two large and highly polar cyano groups, which should

lead to a larger intermolecular separation than that of the corresponding difluoro-substituted analogue (**14**). Hence the dinitrile (**15**) does not exhibit any observable liquid crystalline phases. Compounds (**11** and **16–18**) without lateral substituents exhibit smectic phases with much higher liquid crystalline transition temperatures than those of the 2,3-difluoro-substituted terphenyl (**14**) and the 2,3-dicyano-substituted terphenyl (**15**) due to the absence of steric effects and a lower degree of interannular twisting related to the presence of the lateral substituents. The lateral intermolecular distances will be shorter for compounds (**11** and **16–18**) than those for compounds (**14** and **15**) and hence the intermolecular forces of attractions will be greater. The 2,5-disubstituted pyridine (**16**) and pyrimidine (**17**) exhibit SmA phase. The slight asymmetry of compounds (**16** and **17**) may contribute to lower melting points than that of the symmetrical terphenyl (**11**). The large transversal dipole moment attributed to the two nitrogen atoms present in the 2,5-disubstituted pyridazine (**18**) and the symmetrical structure result in an almost identical melting point to that of terphenyl (**11**). A SmA phase is also observed for this aromatic nitrogen heterocycle due to the large lateral forces of attraction between neighbouring molecules of the 2,5-disubstituted pyridazine (**18**).

The substituted 4-pentyl-*p*-terphenyls (**19–29**) also collated in Table 4 each possess a *n*-pentyl-chain in a terminal position of the aromatic core and a fluoro- or cyano-substituent in the other terminal position, as well as, in most cases, a number of fluoro-substituents in various lateral positions. It is noted that the presence of a fluoro-substituent in a terminal position rather than a lateral position of compound (**19**), instead of an alkyl group, c.f. compound (**11**), results in the absence of observable liquid crystalline behaviour, although the melting point is high and a monotropic nematic phase could be present. Compound (**20**) possesses one fluorine atom in a lateral position and one in a terminal position. This combination of fluoro-substituents explains the moderately high melting and clearing points of this material, as well as the presence of a SmA phase. The trifluoro substituted compound (**21**) shows a lower melting and clearing point without a smectic phase, compared with the mesomorphic behaviour of the mono-fluoro-substituted compound (**19**). This is probably due to steric effects, rather than differences in the polarity of the molecules. The reference 4-cyano-4''-pentyl-*p*-terphenyl (**22**) (**50**), exhibits a high melting and clearing point partly due the presence of the cyano group with a large dipole moment ($\mu = 4 \text{ D}$) in a terminal position. (**59, 60**) This is known to induce a high degree of molecular interdigitation in the nematic phase, which is partly responsible for the high clearing point (**59, 60**). The presence of one fluorine atom in a

lateral position in compounds (**23** and **24**) results in a lower melting and clearing point than those of compound (**22**) due to steric effects and a higher degree of interannular twisting (**57, 58**). The presence of two fluorine atoms in lateral positions next to a cyano group in a terminal position in 4-cyano-3,5-difluoro-4''-pentyl-*p*-terphenyl (**25**), results in an even lower melting point and clearing point compared with those of the compounds (**22–24**). This is perhaps to be expected taking into account the non-linear shape of compound (**25**) with a low aspect ratio, as shown in Figure 1. There is significant interannular twisting ($\sim 35^\circ$) about the C-C bonds connecting the phenyl rings in the aromatic core of the compound (**25**) as expected.

The 4-cyano-2',3'-difluoro-4''-pentyl-*p*-terphenyl (**26**) exhibits an intermediate clearing point as both fluorine atoms are adjacent and on the same side of the molecule. The large resultant dipole moment orthogonal to the long molecular axis may contribute to the induction of a SmA phase at elevated temperatures. The trifluoro-substituted cyano-*p*-terphenyl (**27**) possesses even lower melting and clearing points and no smectic phase. This can be attributed to the presence of one additional fluorine atom in a lateral position next to the terminal cyano group and a combination of steric effects, a high degree of interannular twisting and a lower degree of intermolecular association (**57–60**). The presence of one more fluorine atom in a lateral position next to the terminal cyano group of 4-cyano-2',3',3,5-tetrafluoro-4''-pentyl-*p*-terphenyl (**28**) results in even lower melting and clearing points and to the absence of a smectic phase. This behaviour is consistent with the above explanations related to steric and electronic effects attributable to fluorine atoms in a lateral position. The pentafluoro-substituted cyano-*p*-terphenyl (**29**), which differs from compound (**28**) by the presence of a fluorine atom in place of the cyano group in a terminal position, does not exhibit an observable mesophase despite considerable supercooling below the melting point. The absence of a cyano group will result in a much lower degree of molecular interdigitation and consequently a much lower effective length-to-breadth ratio compared with that of associated pairs of molecules (**57–60**).

3.2 Physical properties

The reference 4,4''-dipentyl-*p*-terphenyl (**11**) and the substituted 4,4''-dipentyl-*p*-terphenyls (**12–15**), the nitrogen heterocycles (**16–18**) and the substituted 4-pentyl-*p*-terphenyls (**19–29**) collated in Table 4 are rigid and consist of three six-membered aromatic rings in a linear configuration with one or two pentyl chains in *para*-positions situated on the terminal

phenyl rings, often with one or more fluoro- or cyano-substituents in terminal or lateral positions. Several compounds listed in Table 4 are not soluble enough to make up the test mixtures; for example, the reference 4,4''-dipentyl-*p*-terphenyl (**11**), which is apolar and exhibits a high melting point, is missing from Table 2 for this reason. The solubility of individual compounds in different nematic mixtures is difficult to predict. For example, the 2,3-difluoro-4,4''-dipentyl-*p*-terphenyl (**14**) is polar, although of negative dielectric anisotropy, and exhibits a low melting point. However, it is not soluble enough in the host nematic mixture MLC-6437-000, which is also very polar, but of positive dielectric anisotropy, and had to be replaced by the more soluble 2',3'-difluoro-4-ethyl-4''-pentyl-*p*-terphenyl (**30**) (see Table 2). The 4-fluoro-4''-pentyl-*p*-terphenyl phenyl (**19**), although expected to exhibit a small positive value of the dielectric anisotropy, possesses a very high melting point and is also not soluble in the host nematic mixture, and is also absent from Table 2 along with others for similar reasons.

Compounds (**12**, **13**, **16** and **30**) are of zero or negative dielectric anisotropy and lead to lower values of dielectric anisotropy ($\Delta\epsilon$) of the guest–host nematic mixtures as expected (see Table 2). The presence of compounds (**12**, **13**, **16** and **30**) as dopants in the host nematic mixture leads to higher values of the splay and bend elastic constants (k_1 , k_3), and therefore the average elastic constant (κ) for the resultant guest–host mixture, than those of the host mixture MLC-6437-000. The presence of 8 wt% of any of the compounds (**12**, **13**, **16** and **30**) as dopants in the guest–host nematic mixture reduces the magnitude of $\bar{\epsilon}/\kappa$ and $\bar{\epsilon}$ compared with the values for the non-doped host mixture MLC 6437-000. It should be noted that an increase, rather than a reduction, in $\bar{\epsilon}/\kappa$ on addition of the dopant (**30**) from $0.6 \text{ C m}^{-1} \text{ N}^{-1}$ to $2.2 \text{ C m}^{-1} \text{ N}^{-1}$ at a concentration of 8 wt% to the nematic mixture E7, composed of cyanobiphenyls and terphenyls, was observed previously (22). It is possible that in this case the increase in $\bar{\epsilon}/\kappa$ could be due to a reduction in the percentage of polar molecules in the host mixture in an interdigitated dimer arrangement (59, 60). This is the basis of creating multiplexable mixtures for TN-LCDs, by the addition of apolar components to polar mixture, such as E7 (61), whereby the dielectric anisotropy of the mixture actually increases, where a reduction, based on a simple addition of dipolar contributions of all mixture components, would be expected. The increase in the dielectric anisotropy is due to a higher percentage of non-interdigitated mixture components of high dielectric anisotropy. Therefore, this would be consistent with the suggestion that the molecular interdigitation of bent

molecular dimers makes an important contribution to the flexoelectric effect in the nematic phase. However, the host mixture MLC-6437-000 is comprised mainly of polyfluorinated liquid crystals and, although the degree of molecular interdigitation to form molecular dimers is not known, it is likely to be low. Therefore, the addition of the dopants may simply dilute the mixture, if no (or only a small percentage of) interdigitated molecular dimers are present. This would explain the reduction in $\bar{\epsilon}/\kappa$ observed in Table 2 on addition of the dopants (**12**, **13**, **16** and **30**). The changes in $\bar{\epsilon}/\kappa$ and $\bar{\epsilon}$ are much larger ($\approx 20\%$), than the degree of dilution, however, and so other effects may have to be taken in account, e.g. the flexoelectric coefficients of these dopants may be of the opposite sign to the host.

The substituted 4-pentyl-*p*-terphenyls (**21** and **23–26**) should exhibit a strongly positive dielectric anisotropy due to the combined presence of polar substituents such as the cyano group or fluoro groups in terminal and lateral positions, and indeed the addition of compounds (**21**, **24** and **25**) to the host nematic mixture MLC-6437-000 gives rise to a significant increase in the dielectric anisotropy of the resultant guest–host mixtures. The change in dielectric anisotropy does not correlate with the clearing point of the mixture, which is sometimes higher and sometimes lower than that of the host mixture MLC-6437-000; i.e. the value of the dielectric anisotropy does not appear to be greatly affected by the order parameter in these cases. In reality the difference in nematic clearing point is too small to significantly affect the order parameter at the temperatures of these measurements. The guest–host mixtures containing the 4-pentyl-*p*-terphenyls (**21** and **23–26**) show a general increase in k_1 and a decrease in k_3 compared with those of the host mixture. The presence of 8 wt% of the dopants (**21** and **23–26**) in guest–host mixtures based on MLC 6437-000 leads to small-to-moderate increases in $\bar{\epsilon}/\kappa$ and $\bar{\epsilon}$ compared with those of the host mixture. Some of these changes are within the experimental error. There is some correlation between the increase in the value of $\bar{\epsilon}/\kappa$ and the increase in the magnitude of $\Delta\epsilon$ of the mixtures, and the highest values are observed for the mixture containing the very polar compound (**25**). Taken together with other data from Table 2 for the mixtures containing much more apolar compounds, this suggests that the presence of polar components of strongly positive $\Delta\epsilon$ gives rise to higher values of $\bar{\epsilon}/\kappa$ and $\bar{\epsilon}$ for nematic mixtures containing them. This is consistent with recently published results describing the effect of dopants of very high positive $\Delta\epsilon$ on the flexoelectric coefficients of the nematic mixtures E7 (23).

Two more host nematic mixtures, E7 and ZLI-4792, were used to test the generality of the finding that the presence of calamitic dopants of positive $\Delta\epsilon$ in guest–host nematic mixtures leads to higher values of \bar{e}/κ than those values of the host nematic mixture itself (MLC-6437-000). The data listed in the Table 3 for guest–host mixtures containing between 2–16 wt% of the dopant (**25**) in each of the nematic host mixtures MLC-6437-000, E7 and ZLI-4792, leads to a corresponding increase in \bar{e}/κ of the doped guest–host mixtures compared with the values for the pure host mixtures, although the increases are not very large. The plots of the dependence of \bar{e}/κ on the concentration of the dopant in the nematic host mixtures E7 and ZLI-4792 are shown together in Figure 2 for comparison. A linear response is observed for both plots, although the gradients of the plots are not identical. The use of three nematic host mixtures MLC-6437-000, E7 and ZLI-4792 with greatly different values of the dielectric anisotropy ($\Delta\epsilon = 18.1, 14.1$ and 5.3 , respectively), suggests that these effects are genuinely due to the flexoelectric effect and not dielectric effects. The increase in the flexoelectric coefficients in E7 may due to a higher percentage of non-interdigitated mixture components of high dielectric anisotropy, which may suggest that the molecular interdigitation of bent molecular dimers makes an important contribution to the flexoelectric effect in the nematic phase. However, this does not explain the changes in the magnitude of the flexoelectric effect in the host MLC-6437-00 and ZLI-4792 mixtures consisting primarily of (non-interdigitated)

polyfluorinated components. However, the overall polarity of the resultant doped mixtures is higher than that of the host mixtures and this may be primarily responsible for the higher values of the flexoelectric ratio. The values for \bar{e}/κ for the guest–host mixtures containing the rod-like compound (**25**) are lower than those of similar mixtures incorporating 10 wt% of highly polar wedge-shaped compounds of similar values of the dielectric anisotropy, but with a much greater shape anisotropy (**23**). Small wedge-shaped molecules of high polarity only induce small increases in similar guest–host nematic mixtures at similar concentrations, although larger banana-shaped molecules induce much larger increases in polar host mixtures (**21, 22**). These results suggest that highly polar molecules with a very pronounced wedge-, pear- or banana-shape or conformation are required to induce a large flexoelectric effect. This observation is consistent with the results observed for highly polar molecular dimers (**17–20**) and is consistent with R. B. Meyer's original postulation (**1**).

4. Conclusion

The presence of a low concentration (8 wt%) of laterally and terminally substituted *para*-terphenyls with a rigid-rod-like shape and of low or negative dielectric anisotropy as dopants in the nematic mixture MLC 6437-000 of positive dielectric anisotropy leads to lower values of \bar{e}/κ . Similar calamitic dopants of positive dielectric anisotropy lead to small-to-moderate increases in \bar{e}/κ when added at the same concentration

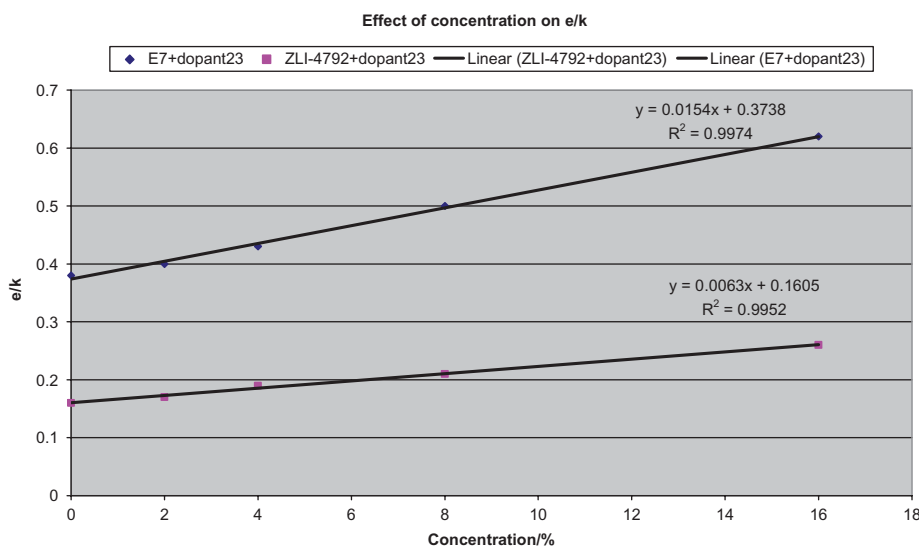


Figure 2. Plot of the effect on e/κ of changes in concentration of 4-cyano-3,5-difluoro-4''-pentyl-*p*-terphenyl (**25**) as a dopant in the commercial nematic mixtures E7 (◆) and ZLI-4792 (■).

to the same nematic host mixture. There is a linear correlation between the concentration of a dopant of high positive dielectric anisotropy and the magnitude of $\overline{\epsilon}/\kappa$ of guest–host nematic mixtures of high positive dielectric anisotropy. The overall polarity of these doped guest–host mixtures is higher than that of the host mixtures and this may be primarily responsible for the higher values of the flexoelastic ratio.

Acknowledgments

We express our thanks to the Merck Chemicals Ltd for funding a PhD studentship (NA). We would also like to thank B. Worthington (^1H NMR) and K. Welham (MS) for spectroscopic measurements.

References

- (1) Meyer, R.B. *Phys. Rev. Lett.*, **1969**, 22, 918–921.
- (2) de Gennes, P.G. *The Physics of Liquid Crystals*, 2nd Edn; Clarendon Press: Oxford, 1992.
- (3) Marinov, Y.; Kosmopoulos, J.; Weissflog, W.; Petrov, A.G.; Photinos, D.J. *Mol. Cryst. Liq. Cryst.*, **2001**, 357, 221–228.
- (4) Marinov, Y.; Naydova, S.; Petrov, A.G. *Bulg. J. Phys.*, **2004**, 31, 28–32.
- (5) Patel, J.S.; Meyer, R.B. *Phys. Rev. Lett.*, **1987**, 58, 1538–1540.
- (6) Rudquist, P.; Komitov, L.; Lagerwall, S.T. *Liq. Cryst.*, **1997**, 23, 503–510.
- (7) Rudquist, P.; Komitov, L.; Lagerwall, S.T. *Phys. Rev. E*, **1994**, 50, 4735–4743.
- (8) Coles, H.J.; Musgrave, B.; Coles, M.J.; Willmott, J. *J. Mater. Chem.*, **2001**, 11, 2709–2716.
- (9) Barberi, R.; Giocondo, M.; Durand, G. *Appl. Phys. Lett.*, **1992**, 60, 1085–1086.
- (10) Dozov, I.; Nobili, M.; Durand, G. *Appl. Phys. Lett.*, **1997**, 70, 1179–1181.
- (11) Bryan-Brown, G.P.; Towler, M.J.; Bancroft, M.S.; McDonnell, D.G. SID (1995); Bryan-Brown, G.; Jones, C.J. Proc. SID '97, Boston, USA, 1997.
- (12) Z.B.D. Limited, Malvern Hills Science Park, Geraldine Road, Malvern, Worcs., WR14 3SZ. Internet address: <http://www.zbdisplays.com>.
- (13) Schmidt, D.; Schadt, M.; Helfrich, W. *Z. Naturforsch.*, **1972**, 27a, 277–280.
- (14) Petrov, A.G.; Th. Ionescu, A.; Versace, C.; Scaramuzza, N. *Liq. Cryst.*, **1995**, 19, 169–178.
- (15) Hermann, D.S.; Komitov, L.; Lagerwall, S.T.; Heppke, G.; Rauch, S. Proceedings of the 27th Freiburg Liquid Crystal Conference, 1998, p 57–1–4.
- (16) Harden, J.; Mbanga, B.; Eber, N. Fodor-Csorba, K.; Sprunt, S.; Gleeson, J.T.; Jakli, A. *Phys. Rev. Lett.*, **2006**, 97, 157802–1–4.
- (17) Musgrave, B.; Lehman, P.; Coles, H.J. *Liq. Cryst.*, **1999**, 28, 1235; *Mol. Cryst. Liq. Cryst.*, **1999**, 328, 309–316.
- (18) Musgrave, B.; Lehman, P.; Perkins, M.J.; Coles, H.J.; *Mol. Cryst. Liq. Cryst.*, **2001**, 366, 735–742.
- (19) Broughton, B.J.; Clark, M.J.; Blach, A.E.; Coles, H.J. *J. Appl. Phys.*, **2005**, 98, 0341109–1–6.
- (20) Coles, H.J.; Clarke, M.J.; Morris, S.M.; Broughton, B.J.; Blach, A.E. *J. Appl. Phys.*, **2006**, 99, 034104–1–6.
- (21) Campbell, N.L.; Duffy, W.L.; Thomas, G.I.; Wild, J.H.; Kelly, S.M.; Bartle, K.; O'Neill, M.; Minter, V.; Tuffin, R.P. *J. Mater. Chem.*, **2002**, 12, 2706–2721.
- (22) Wild, J.H.; Kirkman, N.T.; Kelly, S.M.; Bartle, K.; O'Neill, M.; Stirner, T.; Tuffin, R.P. *Chem. Mater.*, **2005**, 17, 6354–6360 and references therein.
- (23) Wild, J.H.; Bartle, K.; O'Neill, M.; Kelly, S.M.; Tuffin, R.P. *Liq. Cryst.*, **2006**, 33, 635–644.
- (24) Hermann, D.S.; Rudquist, P.; Ichimura, K.; Kudo, K.; Komitov, L.; Lagerwall, S.T. *Phys. Rev. E*, **1997**, 55, 2857–2860.
- (25) Ferrarini, A. *Phys. Rev. E*, **2001**, 64, 021710–111.
- (26) Helfrich, W. *Z. Naturforsch.* **1971**, 26a, 833–836.
- (27) Derzhanski, A.I.; Petrov, A.G.; Hinov, H.P.; Markovski, B.L. *Bulg. J. Phys.*, **1974**, 1, 165–172.
- (28) Hinov, H.P. *Bulg. J. Phys.*, **2004**, 31, 55–67.
- (29) Prost, J.; Marcerou, J.P. *J. Phys.*, **1977**, 38, 315–324.
- (30) Osipov, M.A. *Sov. Phys. JETP*, **1983**, 58, 1167–1171.
- (31) Ponti, S.; Zihlerl, P.; Ferrero, C.; Zumer, S. *Liq. Cryst.*, **1999**, 26, 1171–1177.
- (32) Singh, Y.; Singh, U.P. *Phys. Rev. A*, **1989**, 39, 4254–4262.
- (33) Brown, C.V.; Mottram, N.J. *Phys. Rev. E*, **2003**, 68, 31702–1–5.
- (34) Ferrarini, A.; Greco, C.; Luckhurst, G.R. *J. Mater. Chem.*, **2007**, 17, 1039–1042.
- (35) Takahashi, T.; Hashidate, S.; Nishijou, H.; Usui, M.; Kimura, M.; Akahane, T. *Jpn. J. Appl. Phys.* **1998**, 32, 1865–1869.
- (36) Madhusudana, N.V.; Durand, G. *J. Physique Lett.*, **1985**, 46, L195–L200.
- (37) Petrov, A.G. In *Physical Properties of Liquid Crystals Vol. 1: Nematics*. Dunmur, D.A.; Fukuda, A. and Luckhurst, G.R., Eds., EMIS Data Reviews Series; IEE: UK, 2001; **25**, 251–264.
- (38) Warriar, S.R.; Madhusudana, N.V. *J. Phys. II France*, **1997**, 7, 1789–1803.
- (39) Blinov, L.M.; Barnik, M.I.; Ohoka, H.; Shtykov, N.M.; Yoshino, K. *Eur. Phys. J.* **2001**, E4, 183–192.
- (40) Mazzulla, A.; Ciuchi, F.; Sambles, J.R. *Phys. Rev. E*, **2001**, 64, 21708–1–6.
- (41) Jewell, S.A.; Sambles, J.R. *J. Appl. Phys.*, **2002**, 92, 19–24.
- (42) Parry-Jones, L.A.; Elston, S.J. *J. Appl. Phys.*, **2005**, 97, 093515–1–7.
- (43) Tidey, E.K.; Parry-Jones, L.A.; Elston, S.J. *Liq. Cryst.*, **2007**, 34, 251–255.
- (44) Gray, G.W.; Hird, M.; Lacey, D. Toyne, K.J. *J. Chem. Soc., Perkin Trans.* **1989**, 2, 2041–2053.
- (45) Miyaura, N.; Yanagi, T.; Suzuki, A. *Synth. Commun.*, **1981**, 11, 513–519.
- (46) Suzuki, A. *Pure Appl. Chem.*, **1994**, 66, 213–222.
- (47) Suzuki, A. *J. Organometallic Chem.*, **1999**, 576, 147–168.
- (48) Huth, A.; Beetz, I.; Schumann, I. *Tetrahedron*, **1989**, 45, 6679–6682.
- (49) Hird, M.; Toyne, K.J.; Gray, G.W.; McDonnell, D.G.; Sage, I.C. *Liq. Cryst.*, **1995**, 18, 1–11.
- (50) Gray, G.W.; Harrison, K.J.; Nash, J.A. *Chem. Commun.*, **1974**, 431–432.
- (51) Schubert, H.; Lorenz, H.Z.; Hoffmann, R.; Franke, F. *Z. Chem.*, **1966**, 6, 337–338.
- (52) Chan, L.K.M.; Gray, G.W.; Lacey, D. *Mol. Cryst. Liq. Cryst.*, **1985**, 123, 185–204.
- (53) Gray, G.W.; Hird, M.; Toyne, K.J. *Mol. Cryst. Liq. Cryst.*, **1991**, 204, 43–64.

- (54) Demus, D.; Demus, H.; Zschke, H. *Flüssige Kristalle in Tabellen*; VEB Deutscher Verlag für Grundstoffindustrie: Leipzig, 1974.
- (55) Schubert, H.; Zschke, H. *J. prakt. Chem.*, **1970**, 312, 494–506.
- (56) Weygand, C.; Lanzendorf, W. *J. prakt. Chem.*, **1938**, 151, 221–226.
- (57) Hird, M.; Toyne, K.J. *Mol. Cryst. Liq. Cryst.*, **1998**, 323, 1–67 and references therein.
- (58) Coates, D.; Sage, I.C.; Greenfield, S.; Gray, G.W.; Lacey, D.; Toyne, K.J.; Chan, L.K.M.; Hird, M. PCT Int. Pat. Appl. WO 89 12,621 (1984); US Pat. 5,312,563, 1984.
- (59) Leadbetter, A.J.; Richardson, R.M.; Collings, C.N. *J. Physique.*, **1975**, 36, C1–37–44.
- (60) Bordwijk, P. *J. Chem. Phys.*, **1980**, 73, 595–596.
- (61) Bradshaw, M. Raynes, E.P. *Mol. Cryst. Liq. Cryst.*, **1983**, 91, 145–155.